HETRI: Heterogeneous Ising Multiprocessing

Hüsrev Cılasun, Abhimanyu Kumar, Ziqing Zeng, Nafisa Sadaf Prova,
Sachin S. Sapatnekar, Ulya R. Karpuzcu
University of Minnesota, Twin Cities
{cilas001, kumar663, zeng0083, prova026, sachin, ukarpuzc}@umn.edu

Abstract

Ising machines are effective solvers for complex combinatorial optimization problems. The idea is mapping the optimal solution(s) to a combinatorial optimization problem to the minimum energy state(s) of a physical system, which naturally converges to a minimum energy state upon perturbance. The underlying mathematical abstraction, the *Ising model*, can capture the dynamic behavior of different physical systems by mapping each problem variable to a *spin* which can interact with other spins. Ising model as a mathematical abstraction can be mapped to hardware using traditional devices. In this paper we instead focus on *Ising machines* which represent a network of physical spins directly implemented in hardware using, e.g., quantum bits or electronic oscillators.

Each problem variable can interact with another in different ways. Physical connections between pairs of Ising spins capture such variable-to-variable interactions. Spin count for any given type of machine connectivity is subject to fundamental physical limits. Limited-connectivity machines can support arbitrary interaction patterns, but only by using extra physical spins not corresponding to problem variables, which in turn render a larger and oftentimes harder problem for the Ising machine to solve. Ising machines that can directly support generic interactions via all-to-all connectivity, on the other hand, have less number of physical spins than their limited-connectivity counterparts under the same hardware budget. Therefore, larger problems with sparser variable interactions – which fit into limited-connectivity counterparts – can exceed the all-all-connected machine capacity.

No single type of machine connectivity can efficiently cover diverse interaction patterns between problem variables. At the same time, physical limits prohibit arbitrary increases in the physical spin count for any given topology, where problem sizes of practical importance keep growing. To eliminate the scalability bottleneck due to the mismatch in problem vs. Ising machine size and connectivity, in this paper we make the case for HETRI: *Heterogeneous Ising Multiprocessing*. HETRI organizes the maximum number of physical spins that the underlying technology supports in Ising cores; and multiple independent Ising cores, in Ising chips. Ising cores in a chip feature different inter-spin connectivity or spin counts to match the problem characteristics. We provide a detailed design space exploration and quantify the performance in terms of time or energy to solution and solution
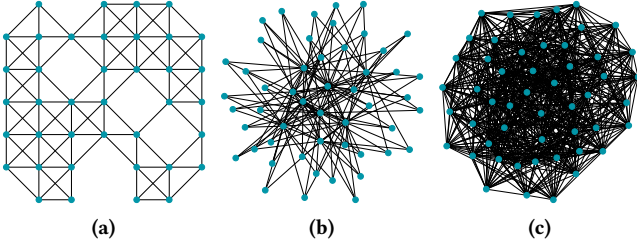
accuracy with respect to homogeneous alternatives under the very same hardware budget and considering the very same spin technology.

1 Introduction

Combinatorial optimization problems represent a broad class of real-world problems with numerous applications in machine learning, robotics or bioinformatics, to name a few. Solving a combinatorial optimization problem translates into finding a configuration that minimizes (or maximizes) an objective function over a discrete search space. Classic solvers tailored for von Neumann machines are NP-complete or NP-hard, hence, the demand for computational resources very quickly increases with growing problem sizes. This is where fundamentally different solver paradigms can help. The Ising model represents a promising alternative mathematical abstraction, which applies to a wide range of physical systems. The model represents the system as a graph, where each vertex corresponds to a spin assuming one of two possible stable states, and where each edge captures the pairwise interaction between two spins. The state of the system corresponds to a binary vector with as many elements as the number of spins. Upon perturbation, physical spins naturally converge to and stabilize at a minimum energy state. Mapping a combinatorial optimization problem to Ising model hence entails translating problem variables to spins; and variable interactions, to spin interactions, respectively, in such a way that the optimal solutions to the combinatorial optimization problem match the minimum energy states of the underlying physical system.

There are many different ways to implement a network of two-state Ising spins in hardware to directly leverage the physical system dynamics, e.g., by using quantum bits [17, 36, 57] or conventional oscillators [33, 55]. We will refer to such Ising solvers as *Ising machines* in this paper. In a generic optimization problem, each variable can interact with another in different ways. In Ising machines, such variable-to-variable interactions and dependencies correspond to actual physical connections between pairs of spins. While problem sizes of practical importance are growing very fast, irrespective of the underlying technology, the maximum number of spins in hardware for any given type of machine connectivity is subject to fundamental physical limits.

The type of machine connectivity dictates the number of physical Ising spins necessary to solve an optimization problem. Ising machines on one end of the spectrum only

Hüsrev Cılasun, Abhimanyu Kumar, Ziqing Zeng, Nafisa Sadaf Prova,
Sachin S. Sapatnekar, Ulya R. Karpuzcu

Figure 1. Representative problem connectivity (variable interaction) graphs: (a) Planar MIS (Maximum Independent Set), (b) 3SAT (Satisfiability), (c) nonplanar MIS. Each dot corresponds to a spin; and each edge, to a non-zero interaction strength. MIS is a graph problem where the goal is to maximize the number of vertices in an *independent set*, i.e., a set of vertices with no edges connecting its elements. SAT is after finding values of Boolean variables that render a given Boolean formula logic 1. In planar MIS, graph connectivity is limited to nearest neighbors in a mesh. Nonplanar MIS has no limitation.

implement nearest-neighbor spin interactions on a planar grid. Such limited-connectivity machines can support arbitrary interaction patterns only by using extra physical spins. Extra physical spins do not have a direct correspondence to problem variables but impose extra constraints, which typically results in a larger and harder problem for Ising hardware to solve, incurring a higher time or energy to solution and oftentimes a lower solution quality. Ising machines that can directly support generic interactions via all-to-all connectivity, on the other hand, typically incorporate much less physical spins than their limited-connectivity counterparts under the same hardware budget. As a result, for larger problems with sparser variable interactions, the required number of physical spins – which can fit into a sparsely connected alternative machine featuring more spins – becomes more likely to exceed the machine capacity, which can significantly hurt scalability to larger problems.

Typically, the required number of physical spins to map a given problem remains larger than the actual problem variable count, and with increasing problem sizes, can easily exceed machine capacity. Therefore, decomposing the problem into subproblems (that we can represent using the available number of physical spins) becomes necessary. Decomposition by itself is a complex task due to data dependencies between subproblems, which often manifest themselves as conflicting variable assignments (i.e., spin configurations). Mismatches in the problem vs. hardware connectivity directly or indirectly render even more physical spins necessary for problem mapping, further challenging problem decomposition.

As showcased in in Fig.1, combinatorial optimization problems of practical importance come with diverse interaction patterns, and a rigid network topology in hardware cannot efficiently cover all. Moreover, physical limits prohibit arbitrary increases in the physical spin count for any given topology, where problem sizes of practical importance keep growing. One typical limit is due to the degradation of spin-to-spin interactions in hardware with the actual physical distance between spins – where the Ising model expects the same range for interaction strength between any two spins, irrespective of where they physically reside. Another obvious limit for machines implementing spins as quantum bits is quantum noise. The bottom line is: While a different limit to physical spin count, N_{max}, applies for each technology, an N_{max} exists for each technology and is very unlikely to keep up with increasing problem sizes.

To eliminate the scalability bottleneck due to the mismatch in problem vs. Ising machine size and connectivity, in this paper we make the case for HETRI: Heterogeneous Ising Multiprocessing. HETRI organizes the maximum number of physical spins that the underlying technology supports (N_{max}) in Ising cores; and multiple independent Ising cores, in Ising chips. Each HETRI chip incorporates a mix of Ising cores of diverse physical characteristics (such as spin count or inter-spin connectivity) to best match the diverse computational needs of emerging combinatorial optimization problems of practical importance. HETRI can thereby reduce the pressure on problem decomposition, as well as the extra number of physical spins necessary to map a given problem. Combining strengths of various types of Ising machines, HETRI is fundamentally different than state-of-the-art homogeneous designs.

In the following, we provide a detailed design space exploration for architectural composition, and quantify the performance of different design options in terms of time or energy to solution and solution accuracy with respect to homogeneous alternatives under the very same hardware budget and considering the very same spin technology. Section 2 covers the background; Section 3, design space exploration; Section 4 and 5, quantitative analysis; Section 6 related work; and Section 7, summary and discussion of our findings.

2 Background
Ising Model
[3, 4, 18, 19] is a mathematical abstraction, originally introduced in the 1920s for ferromagnetic materials, representing a material as a collection of molecules. Each molecule has a spin, either aligned or anti-aligned with an external magnetic field, where spins may interact with each other in a pairwise manner. A Hamiltonian function captures the energy of an n-spin system with $s = [s_1, s_2, ..., s_n]$ as:

$$H(s) = - \sum_{<i \neq j>} J_{ij} s_i s_j - \sum_i h_i s_i \text{ with } i, j \in [1, 2, ..., n]$$

s_i, the spin of the ith molecule, can be either -1 or $+1$. h_i captures the strength of the *local* field at the ith molecule; J_{ij}, of the *interaction* field between neighboring spins i and j. h_i and J_{ij} are real-valued constants.

The system converges to lower energy states – as characterized by specific configurations of the binary s vector – that minimize $H(s)$ at equilibrium. To establish equilibrium, if J_{ij} is (negative) positive, neighboring spins become (anti-) aligned, i.e., $(s_i s_j = -1)$ $s_i s_j = +1$, rendering a positive product term $J_{ij}s_i s_j$ to minimize $H(s)$. Spins reside in a finite-dimensional lattice, visualized by a generic graph. Ising model applies to any physical system composed of discrete elements (such as spins) interacting in a pairwise fashion [26] and is isomorphic to Quadratic Binary Optimization (QUBO), which is characterized by

$$H(\mathbf{x}) = \mathbf{x}^T Q \mathbf{x} \text{ where } x_i = (s_i + 1)/2$$

$$h_i = Q_{ii}/2 + \sum_{j=1}^{n}(Q_{ij} + Q_{ji})/4 \text{ and } J_{ij} = Q_{ij}/4$$

for $\mathbf{x} = [x_1, \cdots, x_n]^T \in \{0, 1\}^n$ and $Q \in \mathbb{R}^{n \times n}$ for n spins.

Problem formulation reduces to translating problem variables into binary-valued spins; and problem constraints, into pairwise interaction (J_{ij}) and local field (h_i) strengths. Many important NP-complete/hard problems, including all of Karp's 21 NP-complete problems, have been formulated according to the Ising model [34]. The goal is having the minimum energy state(s) encode the optimal solution(s). If this is the case, by construction, any (e.g., thermally) disturbed physical system that complies with the Ising model, with very high probability, can solve a complex combinatorial optimization problem by converging to a solution at (thermal) equilibrium [6]. We also need to define how $H(s)$ (and individual spin states) evolve over time, which is not captured by the basic mathematical model. For a given optimization problem, different Ising or QUBO fomulations may exist. Ising or QUBO models primarily capture pair-wise interactions between spins, hence problem variables. However, more variables than a mere two may interact with each other in a generic combinatorial optimization problem. This, for instance, is the case for 3SAT(isfiability), a standard combinatorial optimization problem where the goal is finding an assignment of N problem variables (X) that sets a Boolean function $f(x_1, \cdots, x_n)$ to logic 1. In Conjuctive Normal Form (CNF),

$$f(x_1, \cdots, x_n) = C_1 \wedge C_2 \wedge \cdots \wedge C_m \text{ with } X = \{x_1, \cdots, x_n\}$$

applies, where each clause $C_i = l_1 \vee l_2 \vee l_3$ is a disjunction of at most three literals $l_1, l_2, l_3 \subset X \cup \neg X$. For problems like 3SAT, different mathematical formulations differ in how they translate higher order (problem variable) interactions to pairwise (spin) interactions by using ancillary variables, which typically results in a larger problem than the actual problem. Here is an example for a compact 3SAT QUBO formulation

[10] [1]:

$$H(\mathbf{x}) = \sum_{i=0}^{m-1}(-(x_a+1)(x_1+x_2+x_3)+2x_a+x_1x_2+x_1x_3+x_2x_3)$$

m represents the number of clauses. x_1, x_2, and x_3 are Boolean variables in a 3SAT clause (or their inverses $1-x_\bullet$ depending on the polarity of the literals). An ancillary variable x_a is added for each clause to capture energy levels corresponding to third-order interactions. This formulation results in an $(m+n)$ variable problem for an original problem with m clauses and n problem variables.

Ising Model based solvers in software and hardware follow different approaches in implementing convergence dynamics. Growing problem sizes of emerging combinatorial optimization problems prohibit exhaustive search, i.e., tabulating $H(s)$ for all possible values of s (which form the search space) to find an optimal solution. Solvers in software typically rely on probabilistic pruning of the search space by using variants of simulated annealing [30], which boils down to probabilistic flipping of selected spin states at each step of search following predefined convergence criteria. Solvers in hardware form two broad classes: The first class [2, 22, 38, 52, 54, 58] treats the Ising model as a pure mathematical abstraction, and adopts the exact same approach as the software solvers to implement system dynamics, except in hardware. The second class of hardware solvers, on the other hand, directly implement Ising model compliant physical systems, and span quantum [17, 27] and quantum-inspired designs [14, 16, 25, 33, 37, 42]. The underlying physical system naturally determines the time evolution of spin states. We focus on the second class in this paper, which we refer to as *Ising machines*. Ising machines primarily differ from each other by their physical connectivity.

Problem decomposition into smaller subproblems is often inevitable, as more spins may become necessary than an Ising machine can support with growing problem sizes. *Subject to fundamental physics, Ising machine spin count for any given network topology cannot increase indefinitely.* Decomposition is a computationally complex task. Depending on the problem, finding a perfect decomposition into independent subproblems may not always be possible. Having overlapping problem variables among subproblems only complicates the matter. Accordingly, many decomposition approaches have to rely on approximations and iterative heuristics with each iteration dedicated to one subproblem.

For each subproblem that spans as many physical spins as the underlying Ising machine can support, a key question becomes how to account for the impact of the rest of the variables, not covered by the subproblem at hand. One common practical approach is setting the corresponding spins in the Ising formulation of the problem to known values, which is often referred to as *clamping*. Such known values typically

---

[1]Clause specific index parameters omitted to ease illustration.

come from solutions in previous iterations which solved subproblems covering the left-out spins. If for instance, a subproblem covers spin s_j, but not s_i, by setting s_i to (-)1, the $J_{ij}s_is_j$ term would reduce to (-)$J_{ij}s_j$, which we can account for, without breaking the Ising formulation, by updating the local field coefficient h_j to (-)$J_{ij} + h_j$.

Ising solvers are probabilistic in nature. Solvers iterate over multiple, possibly overlapping subproblems to cover all problem spins and try to solve each subproblem a preset number of times. The decomposition algorithm dictates how problem variables get picked in forming subproblems, which has a big impact on solver performance. Decomposition by divide and conquer is common, and variants

either ignore [46] or consider problem connectivity [13].

> *The goal of decomposition is generating* **independent** *subproblems or approximations thereof by having potential inter-subproblem data dependencies absorbed into the mathematical formulation. From the perspective of the Ising hardware, each subproblem is an* **independent** *problem (be it approximately independent or not) that uses as many spins as the machine can support. Accordingly, subproblems generated by a decomposer, even if approximately independent, do not need to communicate with each other directly in the traditional sense.*

3 Heterogeneous Ising Multiprocessors

Macroscopic View: Physical connectivity of hardware spins in an Ising machine can take different forms – even for the same technology to implement spins. From a theoretical perspective, any topology that can support pairwise spin-interactions irrespective of the actual physical location of the two spins works. In the end, implementing the interaction strength J_{ij} requires a physical connection between the spins. Ising machines that support all-to-all connectivity feature a physical link between any pair of spins and can directly map arbitrary J_{ij}. An Ising machine with nearest neighbor connectivity (be it nearest six [1] or nearest four [60]), on the other hand, may not always have a direct physical connection between any arbitrary spin i and j. If this is the case, the machine has to establish the connection by using its available physical links. This is formally referred to as the *embedding* problem in graph theory. Dedicated embedding algorithms [49, 50] exist, but are typically NP-complete/hard. Therefore, the computational overhead of *exact* embedding by itself can dominate the time or energy to solution.

A more practical, *approximate* approach [6] is using multiple *physical* spins to implement a *logical* spin, as illustrated in Fig.2. Fig.2(a) shows the graph corresponding to the generic Ising formulation of an example optimization problem consisting of 5 *logical* spins; Fig.2(b), an embedding on an Ising machine which implements a network of *physical* spins of a specific topology. In Fig.2(b), each of the 2 neighboring *physical* spins labeled s_2 represents a replica of the *logical* spin s_2

from Fig.2(a). To make this work, all physical spins replicating the same logical spin must preserve the very same spin state throughout the computation, which we can achieve by imposing the maximum interaction strength between any such replica. Satisfying this condition, however, becomes harder for larger number of replicas where non-ideal physical effects such as noise start to become significant, which in turn can degrade solution accuracy and/or slow down convergence [9, 23, 31]. Embedding efficiency depends on problem connectivity as well as technology-dependent limits for local replication. In any case, extra spins required for replication taxes the total number of physical spins available to map larger problem sizes.
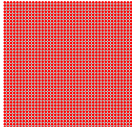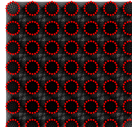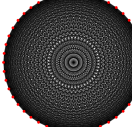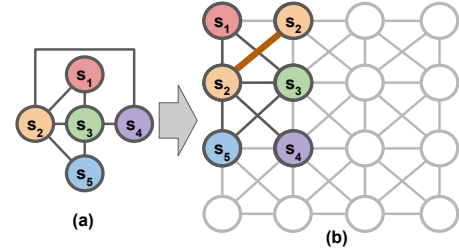

Figure 2. Problem connectivity graph capturing problem variable interactions (a), and its (Ising machine) embedding using node replication (b). Each spin corresponds to a node; each edge in (b), to a physical link.

Machine connectivity dictates the number of physical spins necessary to solve a given optimization problem on an Ising machine. As shown in Table 1, all-to-all connected Ising machines typically have a lower number of physical spins than machines with nearest-neighbor connectivity under the same hardware resource budget, also necessarily considering the very same spin technology. As a result, for problems of sparser connectivity – which can fit into a sparsely connected alternative machine featuring more spins, the required number of physical spins becomes more likely to exceed the machine capacity in an all-to-all connected machine. Many common combinatorial optimization problems such as satisfiability feature sparse problem connectivity (variable interaction) graphs as depicted in Fig.1.

> *A rigid network topology in hardware cannot efficiently cover diverse connectivity patterns of emerging combinatorial optimization problems of practical importance (as demonstrated in Fig.1). Ergo, we are not after an Ising machine that supports a specific topology. Our goal is matching the problem connectivity with machine connectivity in the face of inevitable physical limitations. The efficiency of an Ising machine depends on how well the machine connectivity matches the problem connectivity.*

Microscopic View: For any given technology, a maximum number of spins that can be interconnected to form a functional Ising machine, N_{max}, exists and is a function of the

Connectivity	Sparse (King's Graph)	Hybrid	All-to-all
Number of physical spins (N_{max})	1968	600	48
Area	2.1mm^2	4mm^2	1.8mm^2
Power	42 mW	25 mW	16 mW – 105 mW
Annealing Time	50ns	6400ms	~2500ns
Number of direct physical links per spin	8 (max)	111	47
Technology	65nm CMOS		
Reference	[37]	[35]	[33]

Table 1. Machine connectivity vs. maximum spin count considering the same hardware budget and the very same technology.
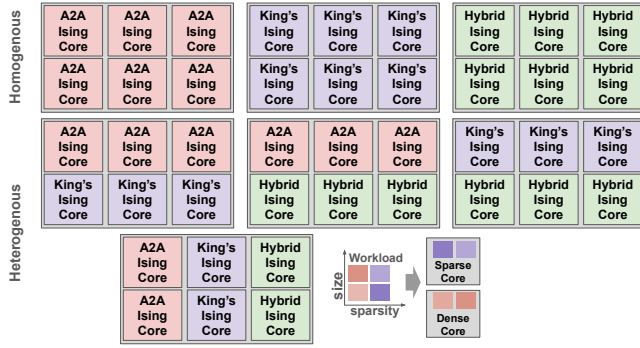
Figure 3. 6-core Ising multiprocessor design space with homogeneous vs. heterogeneous cores.

network topology. We refer to each such network of N_{max} spins as *Ising cores*. For any given optimization problem, the corresponding Ising formulation defines the number of logical spins, $N_{logical}$ necessary to map the problem on an Ising solver. The actual physical number of spins to map the problem, $N_{physical}$, should ideally match $N_{logical}$.

As depicted in Fig.2, *a denser problem connectivity than the machine connectivity* necessitates $N_{physical} > N_{logical}$. Extra physical spins translate into solving a larger and more constrained – and therefore, typically harder – problem in hardware than the actual problem, which usually implies slower convergence to equilibrium and/or lower solution accuracy. At the same time, the likelihood of $N_{physical} > N_{max}$ increases. On the other end of the spectrum, under the same spin technology, a densely connected Ising machine would be able to fit a much lower number of physical spins in the same hardware budget when compared to a sparsely connected machine, rendering a lower N_{max} – as shown in Table 1. Hence, the likelihood of $N_{physical} > N_{max}$ increases with *a sparser problem connectivity than the machine connectivity*, as well. $N_{physical} > N_{max}$ necessitates decomposing the problem into (possibly approximately) *independent* subproblems

that no more than N_{max} physical spins can express, which by itself is a complex task as explained in Section 2.

> *Irrespective of how problem connectivity compares to machine connectivity – for large problems with $N_{logical} > N_{max}$, decomposition is inevitable. Where heterogenous Ising machines can help is eliminate the need for machine-connectivity-induced decomposition for problem sizes which can fit into a given hardware budget as long as the machine connectivity matches the problem connectivity.*

In the following, we discuss how introducing heterogeneity in machine connectivity can help reduce the required number of extra physical spins, and thereby the likelihood of $N_{physical} > N_{max}$, which in turn can render faster convergence to a solution as well as a better solution quality.
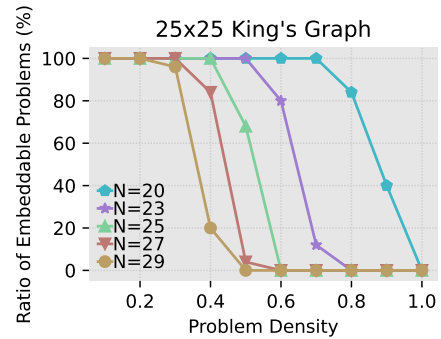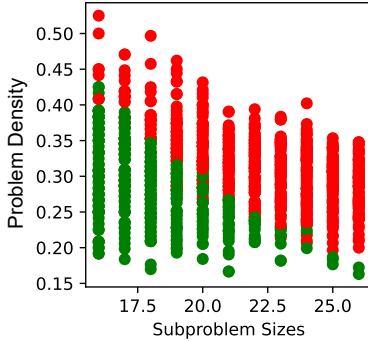

Figure 4. % problems that can be embedded into an Ising core with King's graph connectivity, as a function of problem density (as a proxy for problem connectivity) and problem size in terms of logical number of spins $N = N_{logical}$.

HETRI Design Space: HETRI organizes the maximum number of physical spins that the underlying technology supports in *Ising cores*; and multiple *independent* Ising cores, in Ising chips. A HETRI processor features N_{core} Ising cores per chip, where cores differ from each other primarily by their connectivity. N_{core} for a given technology depends on the hardware

Hüsrev Cılasun, Abhimanyu Kumar, Ziqing Zeng, Nafisa Sadaf Prova,
Sachin S. Sapatnekar, Ulya R. Karpuzcu

(e.g., area) budget. Fig.3 illustrates example 6-core designs featuring a mix of dense (All-to-All, A2A) and sparse (King's graph) Ising cores. In A2A, there is a physical link between any two arbitrary spins. In King's, physical links align with the legal moves of the King chess piece. In Hybrid, physical spins reside in tiles where each tile features 16 all-to-all connected spins and where each tile is connected to all tiles in a 6-tile neighborhood. The Ising core mix for a given N_{core} is a critical design parameter and can span different topologies, not necessarily limited to those shown in Fig.3.

> *As we covered in Section 2, the goal of decomposition is generating independent subproblems or approximations thereof with the mathematical formulation absorbing potential inter-subproblem data dependencies. From the perspective of HETRI each subproblem is an independent problem (be it approximately independent or not) that uses as many spins as an Ising core can support. Accordingly, subproblems – even if approximately independent, do not need to communicate with each other directly in the traditional sense. Ergo, Ising cores do not need to be connected to each other. Physically, we can think of each Ising core as a clustered network of spins, in charge of solving a (sub)problem that best aligns with its connectivity.*

Figure 5. Subproblems of a representative 25-variable 3SAT problem that can(not) be embedded into an Ising core with King's graph connectivity, as a function of density and subproblem size, denoted in green (red).

> *Each Ising core already incorporates the maximum possible number of physical spins that the underlying technology and topology allow in the presence of fundamental physical limits. Under this constraint – which we can fomulate as "each Ising core supporting no less than N_{max} physical spins for a given spin technology and network topology", even if connections between cores were needed (which is not the case by definition), expanding an Ising core with additional physical links would not be possible without breaking functional correctness.*

HETRI does not have a direct correspondent of *(shared) memory* in the conventional sense. In abstract terms, actual

physical states of all spins stitched together would form the equivalent of *architectural state*. Representative quantum or quantum-inspired Ising machines [36, 37, 55] do not use memory or buffers for J_{ij} or h_i values which usually are encoded into physical properties. That said, typical Ising machines deploy small buffers in the conventional sense for reading out the state – such as the scan chain implementations in [33, 37].

As depicted in Fig.1, combinatorial optimization problems come with diverse connectivity patterns, which we can quantify and classify by using conventional metrics from graph theory such as the *ratio of edges to nodes* or the *ratio of edges to the maximum possible number of edges* for a given node count. Even average or maximum *degree* can work, as we are after a ranking of density among (sub)problems rather than an exact calculation – the goal is mapping the densest (sub)problems to the densest Ising cores and vice versa. We can also pre-define a density threshold, and allow only (sub)problems exceeding this threshold to be solved on the densest Ising cores. Beyond the basics, we leave a comprehensive exploration of heterogeneity-aware problem decomposition and (sub)problem mapping to future work.

Matching problem connectivity (as quantified by density) by Ising core connectivity enables larger (sub)problem sizes to be handled by the respective Ising cores without any need for decomposition. Fig. 4 demonstrates this effect for a sparser Ising core featuring a 25×25 King's graph. The x-axis captures problem connectivity using problem density as a proxy. The y-axis shows % randomly generated problems that can be embedded into such an Ising core without decomposition. As problem density increases, embedding becomes impossible for smaller and smaller problems due to the increasing pressure on physical spins. This effect is also visible in Fig. 5, this time considering decomposition, for subproblems of a 25-variable 3SAT problem. For any subproblem size, finding an embedding is less likely for the densest ones. As the subproblem size grows, the share of subproblems that can be embedded very quickly decreases.

4 Evaluation Setup

Simulation Framework: We simulate Ising cores of different connectivity by adapting *tabu search* [41], which represents a general-purpose solver for QUBO/Ising problems. Each *iteration*, the simulator attempts to solve a subproblem that physically fits into the target Ising core. Tabu search is a reliable proxy that does not compromise accuracy at decomposed problem sizes by modeling an Ising/QUBO solver behaviorally. Consequently, it enables accurate architectural simulation at scale to facilitate design space exploration, as opposed to analog simulation[2] of the target Ising cores. The simulator terminates an iteration either upon convergence to

---

[2]We also use a Kuramoto-model based simulator [56] for basic verification, which more accurately captures the convergence dynamics of the target

a solution, or after a timeout limit of 3 milliseconds elapses even if no convergence is the case. We empirically determine the timeout limit by profiling representative combinatorial optimization benchmark problems. To identify the ground truth for each benchmark, however, we increase the timeout limit to 5000 milliseconds.

Problem Decomposition: Without loss of generality, we adapt the Breadth-First Search (BFS) based decomposer from [13], which, as the name implies, iteratively forms a new subproblem by starting from a random root node to expand the subproblem spin by spin through a BF traversal of the problem connectivity graph. Our decomposer thereby ensures that the resulting subproblem connectivity graphs are representative. For each network topology we consider, we let the subproblem size grow spin by spin until it is no longer possible to embed the resulting subproblem in the connectivity graph of the target Ising core. For each configuration, we use the largest possible subproblem. We define *decomposition rate* as the % of spins in the decomposed problem compared to the original problem, and experiment with representative values including the extremes.

Benchmark Problems: We experiment with 3SAT(isfiability) and QUBO (Quadratic Binary Optimization) problems that span a wide spectrum of problem connectivity. 3SAT is one of the first NP-complete problems introduced, often cited as the "original" NP-complete problem [15] with numerous practical use cases, and by definition, can translate into any other NP-complete problem in polynomial time [28]. While we introduced QUBO in Section 2 primarily as an isomorphic mathematical abstraction to the Ising model, it by itself defines a broad class of combinatorial optimization problems with numerous real world applications, as well, where the goal is finding a binary vector that minimizes an objective function. With QUBO being NP-hard and 3SAT NP-complete, our benchmark suite covers multiple graph topologies as well as asymptotic complexity classes. We use 50-spin problems for QUBO and 3SAT. To characterize HETRI for larger scale problems, we also consider 800 Gset benchmarks [62] G11–G16, which represent Max-Cut problems with 800 spins and 1600–4694 weights. As we understandably cannot include each and every combinatorial optimization problem in our analysis, we use benchmark problems from this suite as proxies for common connectivity patterns and representative problem sizes.

We consider three QUBO instances. For the first two, we use Erdős–Rényi (er) and Barabasi-Albert (ba) graph generators from [7], and we sweep parameters p and m, respectively, which manipulate the overall density of the graph. We experiment with $p = \{0.06, 0.12, 0.24, 0.48\}$ and $m = \{1, 2, 4, 8, 16, 32\}$ for Erdős–Rényi and Barabasi-Albert graphs. For the third QUBO instance, we include Power Law

Cluster (pow) graphs from [24] with $p = 0.5$, and run our experiments for $m = \{1, 2, 4, 8, 16\}$. We experiment with 3SAT (sat) benchmarks using the formulation from [10], and include a parametric sweep for $\alpha = \{1, 2, 3, 4, 5\}$, which corresponds to the ratio of the clause count to Boolean variable count in the SAT instance. Fig.s 6a/6b/6c provide example adjacency matrices for Erdős–Rényi graphs with $p = 0.04$, $p = 0.16$, $p = 0.63$; Fig.s 6d/6e/6f, for Barabasi-Albert graphs with $m = 1$, $m = 2$, $m = 8$; Fig.s 6g/6h/6i, for Power Law Cluster graphs with $m = 1$, $m = 4$, $m = 16$; and Fig.s 6j/6k/6l, for 3SAT graphs with $\alpha = 1$, $\alpha = 2$, $\alpha = 5$, respectively, spanning a wide range of density and topologies for problem connectivity.

In the following, we form workloads featuring different mixes of these benchmarks. We thereby can fully control and clearly track the impact of mismatches between problem and machine connectivity on the overall performance and energy efficiency. If a problem needs to be decomposed, resulting subproblems may feature different connectivity patterns, as well. The connectivity graph for 3SAT from Fig. 6l, for instance, reveals that the first 8 (logical) spins are very densely interacting with each other and therefore, that a subproblem incorporating these spins may better map to a densely connected Ising core. Subproblem connectivity, however, strongly depends on the decomposition strategy, as well. Following the 3SAT example, depending on the specific decomposition algorithm, the first 8 spins may or may not end up in the very same subproblem. To make these effects visible, we experiment with different values of the *decomposition rate*.

HETRI Configurations:

> *This paper is not about the design of a specific type of Ising core. Our contribution is an architecture-level insight that applies to different Ising core designs, irrespective of the underlying technology. The literature is full of interesting Ising machine proposals which can serve as component Ising cores for HETRI, as long as they feature the same technology and significantly different connectivity. Without loss of generality, we base our evaluation on three representative Ising core designs from the literature which satisfy these criteria [33, 35, 37].*

As summarized in Table 1, using the very same technology, all three designs rely on conventional oscillators to represent physical spins, however, when it comes to the connectivity, they span the Ising core connectivity design space: A2A corresponds to the densest possible configuration in theory and practice; King's graph, to one of the sparsest options in practice, while the Hybrid graph provides a tangible middle ground. To be more specific, in All-to-all (A2A) [33] a physical link connects each pair of hardware spins; where King's graph [37] only supports nearest neighbor interactions by providing physical links connecting at most 8 hardware spins together. The Hybrid graph, on the other hand, organizes

---

Ising cores, however, which is not scalable to be deployed in architectural design space exploration as we report in this section.
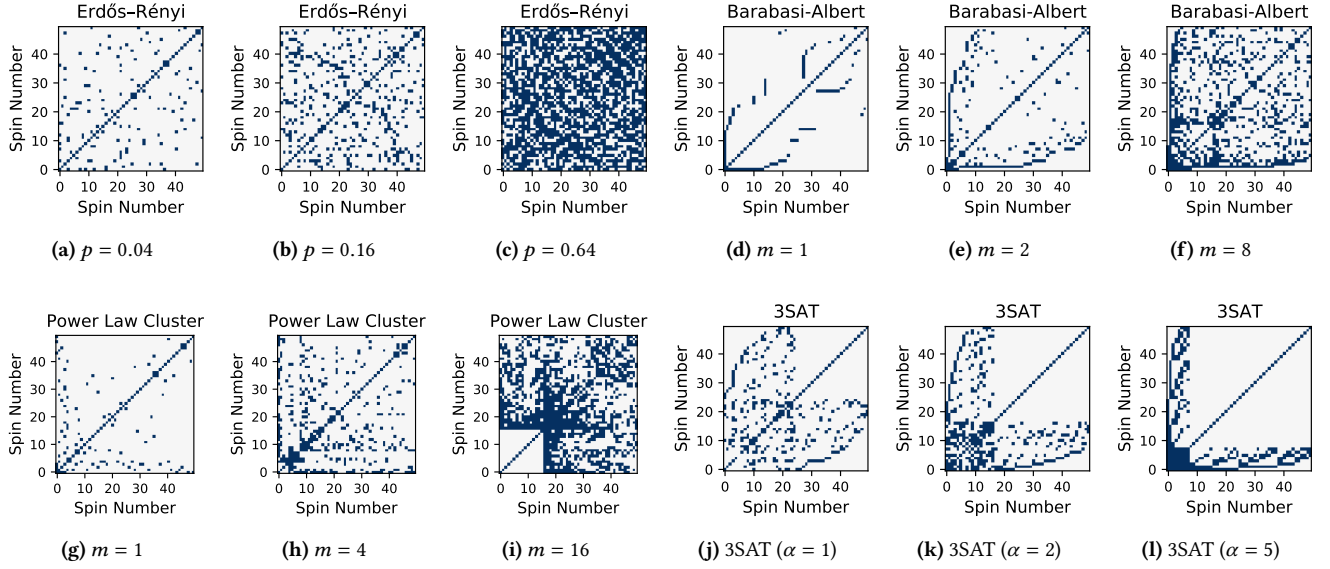
Figure 6. Benchmark problem connectivity as captured by adjacency matrices. x and y axes capture logical spins: (a)/(b)/(c) Erdős–Rényi; (d)/(e)/(f) Barabasi-Albert; (g)/(h)/(i) Power Law; (j)/(k)/(l) 3SAT.

physical spins in tiles where each tile features 16 all-to-all connected spins and where each tile is connected to all tiles in a 6-tile neighborhood. All three of these designs are manufactured and fully characterized, which we leverage in adjusting our simulation parameters for a realistic evaluation. As shown in Fig.3, we experiment with 6-core HETRI multiprocessors and consider 7 (3 homogeneous and 4 heterogeneous) design points: 6 A2A Ising cores; 6 King's Ising cores; 6 Hybrid Ising cores; 3 different HETRI architectures with 6 cores evenly split between two different topologies; and finally an HETRI design with 6 cores evenly split between all three different topologies.

A critical design parameter with direct impact on performance and energy efficiency is the physical spin count per Ising core. Due to topology differences, configuring A2A, Hybrid, and King's Ising cores with the same spin count would be too restrictive. For a fair comparison, we instead allocate the same hardware budget to each core to determine the hardware spin counts, where we fix the hardware budget allocated to physical links implementing pair-wise spin interactions according to a given Ising core topology. The design from [37] featuring $N \times N$ distinct spins that can only interact (couple) with each other in a King's graph fashion is (in terms of coupler cells which establish actual physical connections) iso-hardware-budget with the design from [33] featuring N distinct all-to-all connected spins. We also adjust the parameters from [33] to match the J_{ij} precision of [37] such that our A2A and King's Ising core configurations only differ by connectivity. We experiment with up to 50 (50× 50) spin variants for A2A and King cores. Similarly, we scale

down the 600-spin chip from [35] linearly with the number of couplers to fit 320 spins in a 5×4 grid of 20 tiles, where each tile has 16 all-to-all connected spins.

Metrics: We report *time-to-solution* and *energy-to-solution* which capture the overall execution time and energy consumption, for each problem instance and configuration, until we obtain a solution. To this end, for each problem instance and configuration, we collect from our architectural simulator the type and number of hardware events until we obtain an optimal solution, and associate each with the corresponding time and energy cost from [33, 35, 37] (as summarized in Table 1). Ising machines by construction are probabilistic solvers to combinatorial optimization problems. Therefore, there is no guarantee that each and every attempt results in a solution; some runs may simply terminate without converging to an optimal solution, after the pre-defined timeout limit elapses. For the benchmarks and the configurations considered in the evaluation, we did not encounter such cases. Another key metric for quantitative evaluation of probabilistic solvers is *solution accuracy*, which is a measure of how close the obtained solutions are to the optimal solutions. For 3SAT, a valid solution has to satisfy all clauses – accordingly, we only consider solutions which overlap with ground solutions 100%. We conservatively adapt the same policy also for QUBO problem instances in our benchmark suite. For Gset benchmarks, on the other hand, we set the target solution accuracy to 90%.

Problem scheduling: We experiment with different problem mixes and characterize the behavior under full utilization vs. only one core being active at a time. We use a greedy
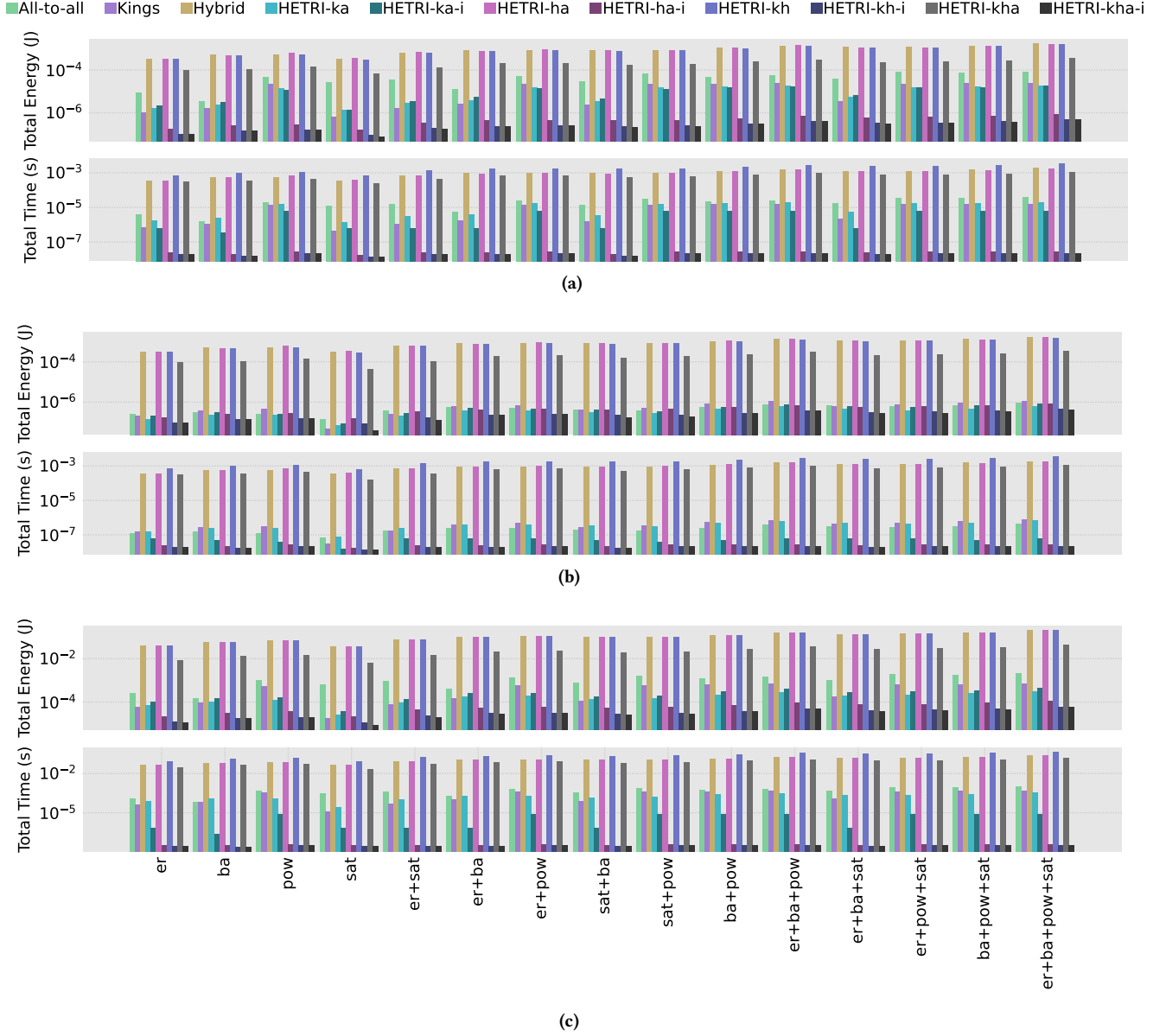
Figure 7. Average time- and energy-to-solution for different workload mixes and decomposition rates: (a) limited to 20%; (b) limited to 84%, and (c) full range (linearly spaced between 20% - 100%).

(sub)problem-to-Ising core assignment policy where the goal is – when possible based on Ising core availability – matching (sub)problem connectivity with Ising core connectivity to maximize performance and energy efficiency. Once mapping completes, each Ising core repetitively solves a (sub)problem until termination. For QUBO, we base the termination criterion on a comparison of the Hamiltonian after each iteration against the ground Hamiltonian. For 3SAT, all clauses in the (sub)problem instance have to be satisfied. For Gset benchmarks we try to reach 90% of the energy of the best-known cut value as the termination criterion.
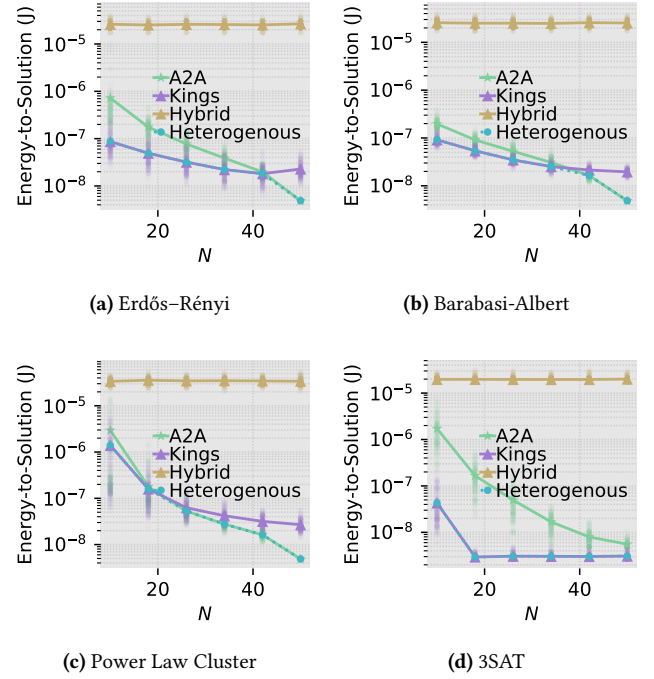
5 Evaluation

We first report time- and energy-to-solution for representative workload mixes, considering different decomposition rates, in Fig. 7: Fig. 7a for 20% decomposition rate; Fig.7b, for 84% decomposition rate; and Fig.7c, for decomposition rates varying between 20% to 100%, respectively. We consider a 6-core HETRI multiprocessor as explained in Section 4. Any configuration labeled as HETRI incorporates a mixture of A2A, Hybrid, and King's Ising cores. HETRI-ka, HETRI-ha,

(a) Erdős–Rényi

(b) Barabasi-Albert

(c) Power Law Cluster

(d) 3SAT
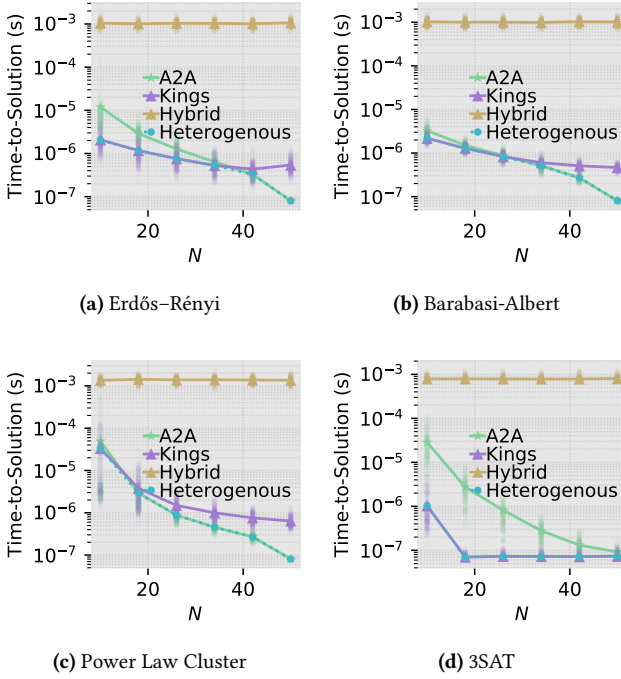
Figure 8. Time-to-solution vs. N for an $N \times N$ array of spins, which translates into N ($N \times N$) physical spins for A2A (King) Ising cores. The x-axis can also be regarded as a proxy for subproblem size, where larger subproblem sizes result in a lower number of iterations, which in turn translates into better performance.

(a) Erdős–Rényi

(b) Barabasi-Albert

(c) Power Law Cluster

(d) 3SAT

Figure 9. Energy-to-solution vs. N. for an $N \times N$ array of spins, which translates into N ($N \times N$) physical spins for A2A (King) Ising cores. The x-axis can also be regarded as a proxy for subproblem size, where larger subproblem sizes result in a lower number of iterations, which in turn translates into lower energy.

and HETRI-kh correspond to systems featuring only 2 different topologies; King's and A2A ; Hybrid and A2A; and King's and Hybrid, respectively. HETRI-kha is the system where all three topologies are present. For each case, -i variants denote the ideal configuration where infinitely many cores are available, to capture the minimum possible time and energy for each configuration. *Overall, when compared to homogeneous alternatives, we observe that HETRI configurations with A2A and King's graphs represent the most effective in matching the (sub)problem connectivity, and generally deliver (or match) the best time and energy to solution as a result. Be it homogeneous or heterogeneous, configurations featuring Hybrid perform the worst as A2A and King's topologies better match individual subproblem connectivities than Hybrid.*

However, several exceptions apply. For 3SAT, at all decomposition rates, the homogeneous Ising multi-core with King's graph topology outperforms HETRI significantly. This effect is also clearly visible in Fig. 7c for any workload mix including 3SAT. The main reason is the extreme problem sparsity of 3SAT, where each clause introduces an ancillary variable that is connected to only three spins. Not surprisingly, the extreme problem sparsity in this case favors the

most sparsely connected Ising multi-core, which is the homogeneous design with all cores featuring the King's graph topology. HETRI multi-core also features Ising cores with King's graph topology, however, not as many as the homogeneous alternative. Therefore, once all of the King's Ising cores are occupied in the HETRI-ka multi-core, the remaining subproblems of extreme sparsity get mapped on A2A cores which incorporate the densest possible topology, and both the performance and energy start to degrade after this point due to the severe mismatch between subproblem vs. Ising core connectivity. In this particular case, the winner will always be the homogeneous design featuring more King's Ising cores.

HETRI can match subproblem connectivity subject to the availability of its cores of respective connectivity. While increasing core count (for each type of connectivity), diversifying connectivity beyond the two extremes (and Hybrid) we consider, or introducing availability-awareness to problem scheduling all may help with this performance pathology, this is a fundamental limitation of HETRI for workloads heavily skewed toward a specific type of connectivity. Larger problem sizes only emphasize this effect, as revealed by the Gset results from Fig. 10. In this case, HETRI can improve
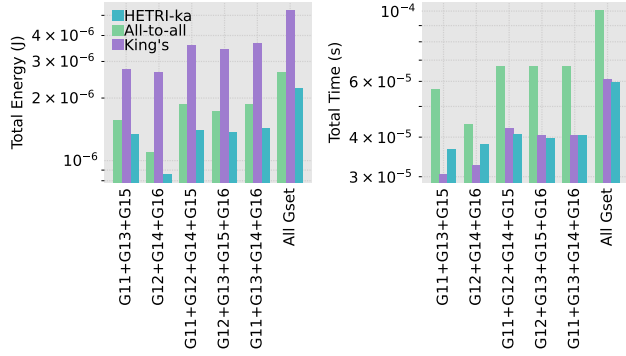
Figure 10. Average time- and energy-to-solution for GSet benchmarks considering different decomposition rates.

energy-to-solution, however, a similar improvement does not apply to time-to-solution due to the limited Ising core count of a specific type of connectivity. To be more specific, G11–G13 have a density of 0.5% (sparse); G14–G16, 1.47% (dense). Aside from skewed mixes (i.e., workload mixes with 2 dense + 1 sparse or 1 dense + 2 sparse benchmarks), HETRI results in a comparable, if not lower, time-to-solution with respect to the homogeneous alternatives.

We should also note that while we sweep the *decomposition rate* in a relatively wide range, the more representative decomposition rates are on the lower end of the spectrum (note that a decomposition rate of 100% indicates no decomposition), rendering the characterization in Fig. 7a as the most representative. This is because, as explained in Section 2, due to fundamental physical limits, no Ising core can increase its physical spin count indefinitely to match growing sizes of emerging combinatorial optimization problems, which necessitates problem decomposition, and only at higher rates.

We next perform a limit study to quantitatively characterize the best case for HETRI multi-cores. For this analysis, irrespective of the number of cores in the Ising multi-core, we solve only one (sub)problem at a time, which translates into only one core being active at a time. Similar to the previous analysis, we experiment with three configurations: two homogeneous multi-cores, one with A2A, the other with King's Ising cores; and a heterogeneous Ising multi-core, where half of the cores are A2A; the other half, King's. Fig. 8 captures the time-; Fig. 9, the energy-to-solution, considering a range of decomposition rates. The figures include all data points, where the trend-lines show the average. The x-axis captures N. We assume an $N \times N$ array of spins, which translates into N ($N \times N$) physical spins for A2A (King's) Ising cores. The x-axis can also be regarded as a proxy for subproblem size, where larger subproblem sizes result in a lower number of iterations, which in turn translates into better performance and energy efficiency. This analysis reveals the break-even points in time- or energy-to-solution

for different configurations. In line with our previous observations, sparser (denser) problems generally perform better on King's (A2A) Ising cores, as they can embed effectively larger problem sizes. While we experiment with different problem densities for 3SAT by sweeping α, 3SAT remains to be a generally sparse problem and always favors King's Ising cores, regardless of the decomposition rate. Overall, for all benchmark problems, HETRI delivers (or matches) the lowest time- or energy-to-solution in this case, by combining best of the both worlds in terms of Ising core connectivity.

6 Related Work

As explained in Section 2, Ising model based solvers in hardware come in two flavors: (1) Solvers that treat the Ising model as a pure mathematical abstraction [2, 12, 22, 38, 45, 51, 52, 54, 58, 61]. (2) Solvers that directly implement Ising model compliant physical systems, including quantum [17, 27] and quantum-inspired designs [14, 16, 25, 33, 37, 42, 46]. Solvers from the first class are out of scope for our paper, which investigates the impact of physical connectivity in hardware. We can think of each solver from the second class, on the other hand, as a component Ising core of a specific connectivity in the context of heterogeneous Ising multiprocessors.

While our approach is not bound to any specific technology, efficient technology-specific solutions to scalability also exists [29, 46, 54], which mostly remain orthogonal to the design options proposed in our paper – suggesting that the underlying techniques can be composable. Still, scalability remains challenging. Efforts in this direction include multi-chip Ising machines [29, 46, 54, 59]; more efficient problem decomposition strategies [13, 53]; more compact problem formulation [11, 39, 40, 43, 48, 63]; exploration of models that can natively support higher order interactions [5, 8, 21, 47]; or hardware connectivity/precision optimization [32, 33, 44].

7 Conclusion

In this paper we make the case for HETRI, heterogeneous Ising multi-cores where each independent core features a different type of connectivity to best match the diverse connectivity spectrum of important combinatorial optimization problems. We quantitatively compare time and/or energy to solution at iso-(solution)-accuracy to homogeneous alternatives using representative benchmark problems, and conduct a detailed sensitivity study to explore the design space.

The key contribution of our paper is an architecture-level insight that applies to different Ising core designs irrespective of the underlying technology. Our effort accordingly is orthogonal to Ising machine design, as we can think of each such design as a component Ising core in our context. Accordingly, we do not cover in grand detail practical implementation aspects which are not specific to heterogeneous designs and which would equally affect homogeneous Ising multi-cores, our baselines for comparison. In this paper, we

focused on integrating multiple Ising cores of the same technology but diverse connectivity into a single chip. Subject to hardware resource budgets expanding the same concept beyond chip boundaries is also possible.
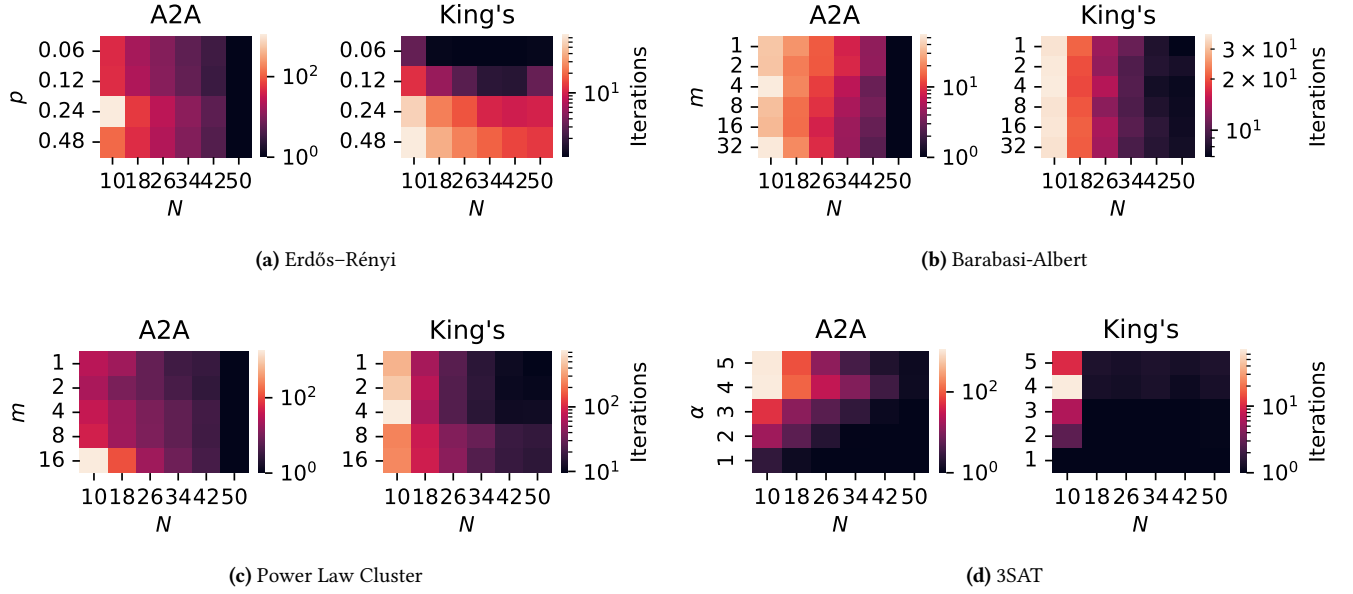
References

[1] Ibrahim Ahmed, Po-Wei Chiu, and Chris H. Kim. 2020. A Probabilistic Self-annealing Compute Fabric based on 560 Hexagonally Coupled Ring Oscillators for Solving Combinatorial Optimization Problems. In *VLSI Symposium.*

[2] Maliheh Aramon, Gili Rosenberg, Elisabetta Valiante, Toshiyuki Miyazawa, Hirotaka Tamura, and Helmut G Katzgraber. 2019. Physics-inspired optimization for quadratic unconstrained problems using a digital annealer. *Frontiers in Physics* 7 (2019), 48.

[3] F. Barahona. 1982. On the computational complexity of Ising spin glass models. *Journal of Physics A: Mathematical and General* 15, 10 (Oct. 1982).

[4] Francisco Barahona, Martin Grötschel, Michael Jünger, and Gerhard Reinelt. 1988. An Application of Combinatorial Optimization to Statistical Physics and Circuit Layout Design. *Oper. Res.* 36, 3 (June 1988), 21 pages.

[5] Mohammad Khairul Bashar and Nikhil Shukla. 2023. Designing Ising machines with higher order spin interactions and their application in solving combinatorial optimization. *Scientific Reports* 13, 1 (2023), 9558.

[6] Zhengbing Bian, Fabián A. Chudak, William G. Macready, and Geordie Rose. 2010. The Ising model: teaching an old problem new tricks. DWave Systems.

[7] Maximilian Böther, Otto Kißig, Martin Taraz, Sarel Cohen, Karen Seidel, and Tobias Friedrich. 2022. What's Wrong with Deep Learning in Tree Search for Combinatorial Optimization. In *International Conference on Learning Representations.*

[8] Connor Bybee, Denis Kleyko, Dmitri E Nikonov, Amir Khosrowshahi, Bruno A Olshausen, and Friedrich T Sommer. 2023. Efficient optimization with higher-order Ising machines. *Nature Communications* 14, 1 (2023), 6033.

[9] Jun Cai, William G. Macready, and Aidan Roy. 2014. A practical heuristic for finding graph minors. arXiv:1406.2741 [quant-ph]

[10] Nicholas Chancellor, Stefan Zohren, Paul A Warburton, Simon C Benjamin, and Stephen Roberts. 2016. A direct mapping of Max k-SAT and high order parity checks to a chimera graph. *Scientific Reports* 6, 1 (2016), 37107.

[11] Zongchen Chen and Elchanan Mossel. 2024. Influence Maximization in Ising Models. arXiv:2309.05206 [cs.DS] https://arxiv.org/abs/2309.05206

[12] Hao-Wei Chiang, Chin-Fu Nien, Hsiang-Yun Cheng, and Kuei-Po Huang. 2024. ReAIM: A ReRAM-based Adaptive Ising Machine for Solving Combinatorial Optimization Problems. In *2024 ACM/IEEE 51st Annual International Symposium on Computer Architecture (ISCA).* IEEE, 58–72.

[13] Hüsrev Cılasun, Ziqing Zeng, Abhimanyu Kumar, Hao Lo, William Cho, William Moy, Chris H Kim, Ulya R Karpuzcu, and Sachin S Sapatnekar. 2024. 3SAT on an all-to-all-connected CMOS Ising solver chip. *Scientific reports* 14, 1 (2024), 10757.

[14] William R Clements, Jelmer J Renema, Y Henry Wen, Helen M Chrzanowski, W Steven Kolthammer, and Ian A Walmsley. 2017. Gaussian optical Ising machines. *Physical Review A* 96, 4 (2017), 043850.

[15] Stephen A Cook. 1971. The complexity of theorem-proving procedures. In *Proceedings of the ACM Symposium on Theory of Computing.* 151–158.

[16] Suryendy Dutta, Abhishek Khanna, AS Assoa, Hanjong Paik, Darrell G Schlom, Zoltán Toroczkai, Arijit Raychowdhury, and Suman Datta. 2021. An Ising Hamiltonian solver based on coupled stochastic phase-transition nano-oscillators. *Nature Electronics* 4, 7 (2021), 502–512.

[17] Sepehr Ebadi, Alexander Keesling, Madelyn Cain, Tout T Wang, Harry Levine, Dolev Bluvstein, Giulia Semeghini, Ahmed Omran, J-G Liu, Rhine Samajdar, et al. 2022. Quantum optimization of maximum independent set using Rydberg atom arrays. *Science* 376, 6598 (2022), 1209–1215.

[18] Edward Farhi, Jeffrey Goldstone, Sam Gutmann, Joshua Lapan, Andrew Lundgren, and Daniel Preda. 2001. A Quantum Adiabatic Evolution Algorithm Applied to Random Instances of an NP-Complete Problem. *Science* 292, 5516 (2001).

[19] Y Fu and P W Anderson. 1986. Application of statistical mechanics to NP-complete problems in combinatorial optimisation. *Journal of Physics A: Mathematical and General* 19, 9 (jun 1986).

[20] Ian P Gent and Toby Walsh. 1994. The SAT phase transition. In *ECAI*, Vol. 94. PITMAN, 105–109.

[21] Alexander W. Glaetzle, Rick M. W. van Bijnen, Peter Zoller, Wolfgang Lechner, Hans Peter Buchler, Marcello Dalmonte, and Guido Pupillo. 2017. A coherent quantum annealer with Rydberg atoms. *Nature Communications* 8 (2017), 15813. https://doi.org/10.1038/ncomms15813

[22] Hayato Goto, Kotaro Endo, Masaru Suzuki, Yoshisato Sakai, Taro Kanao, Yohei Hamakawa, Ryo Hidaka, Masaya Yamasaki, and Kosuke Tatsumura. 2021. High-performance combinatorial optimization based on classical mechanics. *Science Advances* 7, 6 (2021), eabe7953.

[23] Ryan Hamerly, Takahiro Inagaki, Peter L. McMahon, Davide Venturelli, Alireza Marandi, Tatsuhiro Onodera, Edwin Ng, Carsten Langrock, Kensuke Inaba, Toshimori Honjo, Koji Enbutsu, Takeshi Umeki, Ryoichi Kasahara, Shoko Utsunomiya, Satoshi Kako, Ken ichi Kawarabayashi, Robert L. Byer, Martin M. Fejer, Hideo Mabuchi, Dirk Englund, Eleanor Rieffel, Hiroki Takesue, and Yoshihisa Yamamoto. 2019. Experimental investigation of performance differences between coherent Ising machines and a quantum annealer. *Science Advances* 5, 5 (2019), eaau0823. https://doi.org/10.1126/sciadv.aau0823 arXiv:https://www.science.org/doi/pdf/10.1126/sciadv.aau0823

[24] Petter Holme and Beom Jun Kim. 2002. Growing scale-free networks with tunable clustering. *Physical review E* 65, 2 (2002), 026107.

[25] Takahiro Inagaki, Yoshitaka Haribara, Koji Igarashi, Tomohiro Sonobe, Shuhei Tamate, Toshimori Honjo, Alireza Marandi, Peter L McMahon, Takeshi Umeki, Koji Enbutsu, et al. 2016. A coherent Ising machine for 2000-node optimization problems. *Science* 354, 6312 (2016), 603–606.

[26] E Ising. 1925. Beitrag zur theorie des ferromagnetismus. *Zeitschrift für Physik* 31 (1925), 253–258.

[27] M. W. Johnson, M. H S Amin, S. Gildert, T. Lanting, F. Hamze, N. Dickson, R. Harris, A. J. Berkley, J. Johansson, P. Bunyk, E. M. Chapple, C. Enderud, J. P. Hilton, K. Karimi, E. Ladizinsky, N. Ladizinsky, T. Oh, I. Perminov, C. Rich, M. C. Thom, E. Tolkacheva, C. J S Truncik, S. Uchaikin, J. Wang, B. Wilson, and G. Rose. 2011. Quantum annealing with manufactured spins. *Nature* 473, 7346 (May 2011). https://doi.org/10.1038/nature10012

[28] Richard M. Karp. 1972. Reducibility Among Combinatorial Problems. In *Complexity of Computer Computations.* Plenum Press, New York, NY, 85–103.

[29] Tomoya Kashimata, Masaya Yamasaki, Ryo Hidaka, and Kosuke Tatsumura. 2024. Efficient and Scalable Architecture for Multiple-Chip Implementation of Simulated Bifurcation Machines. *IEEE Access* 12 (2024), 36606–36621. https://doi.org/10.1109/access.2024.3374089

[30] S. Kirkpatrick, C. D. Gelatt, and M. P. Vecchi. 1983. Optimization by Simulated Annealing. *Science* 220, 4598 (1983), 671–680.

[31] Mario S. Könz, Wolfgang Lechner, Helmut G. Katzgraber, and Matthias Troyer. 2021. Embedding Overhead Scaling of Optimization Problems in Quantum Annealing. *PRX Quantum* 2 (Nov 2021), 040322. Issue 4. https://doi.org/10.1103/PRXQuantum.2.040322

[32] Santosh Kumar, He Zhang, and Yu-Ping Huang. 2020. Large-scale Ising emulation with four body interaction and all-to-all connections.

Communications Physics 3, 1 (2020), 108.

[33] Hao Lo, William Moy, Hanzhao Yu, Sachin Sapatnekar, and Chris H. Kim. 2023. An Ising solver chip based on coupled ring oscillators with a 48-node all-to-all connected array architecture. *Nature Electronics* 6, 10 (01 Oct 2023), 771–778. https://doi.org/10.1038/s41928-023-01021-y

[34] Andrew Lucas. 2014. Ising formulations of many NP problems. *Frontiers in Physics* 2 (2014).

[35] A Mallick, MK Bashar, DS Truesdell, BH Calhoun, and N Shukla. 2021. Overcoming the accuracy vs. performance trade-off in oscillator ising machines. In *2021 IEEE International Electron Devices Meeting (IEDM)*. IEEE, 40–2.

[36] Catherine McGeochand and Pau Farré. 2022. Advantage Processor Overview. https://www.dwavesys.com/media/3xvdipcn/14-1058a-a_advantage_processor_overview.pdf [Accessed 1-13-2025].

[37] William Moy, Ibrahim Ahmed, Po-wei Chiu, John Moy, Sachin S Sapatnekar, and Chris H Kim. 2022. A 1,968-node coupled ring oscillator circuit for combinatorial optimization problem solving. *Nature Electronics* 5, 5 (2022), 310–317.

[38] Hiroshi Nakayama, Junpei Koyama, Noboru Yoneoka, and Toshiyuki Miyazawa. 2021. Description: third generation digital annealer technology. *Fujitsu Limited: Tokyo, Japan* (2021).

[39] Jonas Nüßlein, Thomas Gabor, Claudia Linnhoff-Popien, and Sebastian Feld. 2022. Algorithmic QUBO formulations for k-SAT and hamiltonian cycles. In *Proceedings of the genetic and evolutionary computation conference companion*. 2240–2246.

[40] Tom Packebusch and Stephan Mertens. 2016. Low autocorrelation binary sequences. *Journal of Physics A: Mathematical and Theoretical* 49, 16 (March 2016), 165001. https://doi.org/10.1088/1751-8113/49/16/165001

[41] Gintaras Palubeckis. 2004. Multistart tabu search strategies for the unconstrained binary quadratic optimization problem. *Annals of Operations Research* 131 (2004), 259–282.

[42] D Pierangeli, G Marcucci, and C Conti. 2019. Large-scale photonic Ising machine by spatial light modulation. *Physical Review Letters* 122, 21 (2019), 213902.

[43] Justo Puerto, Federica Ricca, Moisés Rodríguez-Madrena, and Andrea Scozzari. 2022. A combinatorial optimization approach to scenario filtering in portfolio selection. *Computers & Operations Research* 142 (2022), 105701.

[44] Shruti Puri, Christian Kraglund Andersen, Arne L Grimsmo, and Alexandre Blais. 2017. Quantum annealing with all-to-all connected nonlinear oscillators. *Nature communications* 8, 1 (2017), 15785.

[45] Siddhartha Raman Sundara Raman, Lizy K John, and Jaydeep P Kulkarni. 2024. SACHI: A Stationarity-Aware, All-Digital, Near-Memory, Ising Architecture. In *2024 IEEE International Symposium on High-Performance Computer Architecture (HPCA)*. IEEE, 719–731.

[46] Anshujit Sharma, Richard Afoakwa, Zeljko Ignjatovic, and Michael Huang. 2022. Increasing ising machine capacity with multi-chip architectures. In *Proceedings of the 49th Annual International Symposium on Computer Architecture*. 508–521.

[47] Anshujit Sharma, Matthew Burns, Andrew Hahn, and Michael Huang. 2023. Augmenting an electronic Ising machine to effectively solve boolean satisfiability. *Scientific Reports* 13, 1 (2023), 22858.

[48] Abhishek Kumar Singh, Kyle Jamieson, Peter L. McMahon, and Davide Venturelli. 2022. Ising Machines' Dynamics and Regularization for Near-Optimal MIMO Detection. *IEEE Transactions on Wireless Communications* 21, 12 (2022), 11080–11094. https://doi.org/10.1109/TWC.2022.3189604

[49] J. Su and L. He. 2017. Fast embedding of constrained satisfaction problem to quantum annealer with minimizing chain length. In *2017 54th ACM/EDAC/IEEE Design Automation Conference (DAC)*.

[50] J. Su, T. Tu, and L. He. 2016. A quantum annealing approach for Boolean Satisfiability problem. In *2016 53nd ACM/EDAC/IEEE Design Automation Conference (DAC)*.

[51] Siddhartha Raman Sundara Raman, Lizy K. John, and Jaydeep P. Kulkarni. 2024. SACHI: A Stationarity-Aware, All-Digital, Near-Memory, Ising Architecture. In *2024 IEEE International Symposium on High-Performance Computer Architecture (HPCA)*. 719–731. https://doi.org/10.1109/HPCA57654.2024.00061

[52] Takashi Takemoto, Masato Hayashi, Chihiro Yoshimura, and Masanao Yamaoka. 2019. 2.6 A 2× 30k-spin multichip scalable annealing processor based on a processing-in-memory approach for solving large-scale combinatorial optimization problems. , 52–54 pages.

[53] Siwei Tan, Mingqian Yu, Andre Python, Yongheng Shang, Tingting Li, Liqiang Lu, and Jianwei Yin. 2023. HyQSAT: A hybrid approach for 3-SAT problems by integrating quantum annealer with CDCL. In *2023 IEEE International Symposium on High-Performance Computer Architecture (HPCA)*. IEEE, 731–744.

[54] Kosuke Tatsumura, Masaya Yamasaki, and Hayato Goto. 2021. Scaling out Ising machines using a multi-chip architecture for simulated bifurcation. *Nature Electronics* 4, 3 (2021), 208–217.

[55] Tianshi Wang and Jaijeet Roychowdhury. 2019. OIM: Oscillator-based Ising Machines for Solving Combinatorial Optimisation Problems. In *Unconventional Computation and Natural Computation*, Ian McQuillan and Shinnosuke Seki (Eds.). Springer International Publishing.

[56] Tianshi Wang and Jaijeet Roychowdhury. 2019. OIM: Oscillator-based Ising Machines for Solving Combinatorial Optimisation Problems. arXiv:1903.07163 [cs.ET] https://arxiv.org/abs/1903.07163

[57] Jonathan Wurtz, Alexei Bylinskii, Boris Braverman, Jesse Amato-Grill, Sergio H Cantu, Florian Huber, Alexander Lukin, Fangli Liu, Phillip Weinberg, John Long, et al. 2023. Aquila: QuEra's 256-qubit neutral-atom quantum computer. *arXiv preprint arXiv:2306.11727* (2023).

[58] Kasho Yamamoto, Kazushi Kawamura, Kota Ando, Normann Mertig, Takashi Takemoto, Masanao Yamaoka, Hiroshi Teramoto, Akira Sakai, Shinya Takamaeda-Yamazaki, and Masato Motomura. 2020. STATICA: A 512-spin 0.25 M-weight annealing processor with an all-spin-updates-at-once architecture for combinatorial optimization with complete spin–spin interactions. *IEEE Journal of Solid-State Circuits* 56, 1 (2020), 165–178.

[59] Kasho Yamamoto, Takashi Takemoto, Chihiro Yoshimura, Mayumi Mashimo, and Masanao Yamaoka. 2021. A 1.3-Mbit Annealing System Composed of Fully-Synchronized 9-board x 9-chip x 16-kbit Annealing Processor Chips for Large-Scale Combinatorial Optimization Problems. In *2021 IEEE Asian Solid-State Circuits Conference (A-SSCC)*. 1–3. https://doi.org/10.1109/A-SSCC53895.2021.9634769

[60] M. Yamaoka, C. Yoshimura, M. Hayashi, T. Okuyama, H. Aoki, and H. Mizuno. 2016. A 20k-Spin Ising Chip to Solve Combinatorial Optimization Problems With CMOS Annealing. *IEEE Journal of Solid-State Circuits* 51, 1 (2016).

[61] Guowei Yang, Sina Karimi, Carlos A Ríos Ocampo, Ayse K Coskun, and Ajay Joshi. [n. d.]. SOPHIE: A Scalable Recurrent Ising Machine Using Optically Addressed Phase Change Memory. ([n. d.]).

[62] Y Ye. 2003. Gset max-cut problem set https://web.stanford.edu/yyye/yyye.

[63] Sebastian Zielinski, Jonas Nüßlein, Jonas Stein, Thomas Gabor, Claudia Linnhoff-Popien, and Sebastian Feld. 2023. Pattern QUBOs: Algorithmic construction of 3SAT-to-QUBO transformations. *Electronics* 12, 16 (2023), 3492.

Appendix

Fig. 11 covers the sensitivity of *number of iterations* – the number of times we map a new subproblem to an Ising core – to key problem parameters described in Section 4. By definition, iteration count is a proxy for the effort or cost of solving a (sub)problem, and is closely related to the time- and energy-to-solution reported in Fig. 9 and Fig. 8, respectively.

Hüsrev Cılasun, Abhimanyu Kumar, Ziqing Zeng, Nafisa Sadaf Prova,
Sachin S. Sapatnekar, Ulya R. Karpuzcu

(a) Erdős–Rényi

(b) Barabasi-Albert

(c) Power Law Cluster

(d) 3SAT

Figure 11. Sensitivity of iteration count to problem parameters.

Fig. 11 broadly echoes the observation that N is inversely proportional to the effort or cost of solving a (sub)problem as horizontal magnitude transitions reveal.

Especially for King's Ising cores we observe that the number of iterations is sensitive to other problem parameters, as well: This is the case, e.g., in Fig. 11a and Fig. 11c for Erdős–Rényi and Power Law Cluster graphs.

p (m) is strongly (moderately) correlated with the density in Erdős–Rényi (Power Law Cluster) graphs, where the highest decomposition rate and density yields the maximum iteration count. On the other hand, 3SAT exhibits slightly different characteristics than the QUBO problems, where α=4 incurs the maximum number of iterations. This is in line with the 3SAT transition region with $\alpha \approx 4.2$ [20], where 3SAT problems are considered to be hardest.